

Unified State Feedback Control of a Hybrid Distribution Transformer using Particle Swarm Optimization Tuning

Dave Figueroa*

dave.figueroa.dokt@pw.edu.pl

Alvaro Carreno*

alvaro.carreno@pw.edu.pl

Mariusz Malinowski*

malin@isep.pw.edu.pl

Jun Cheng†

jcheng@gxnu.edu.cn

Zhihong Zhao†‡

zhihongzhao@stu.hit.edu.cn

* Institute of Control and Industrial Electronics, Warsaw University of Technology, Warsaw, Poland.

† Research Institute of Interdisciplinary Intelligent Science, Ningbo University of Technology, Ningbo, China.

‡ Research Institute of Intelligent Control and Systems, Harbin Institute of Technology, Harbin, China.

Abstract—This paper presents a unified state feedback control strategy for a hybrid distribution transformer (HDT) using particle swarm optimization (PSO) for tuning the control gains. The proposed control strategy aims to achieve zero steady-state error for sinusoidal references and disturbances while ensuring good dynamic performance. An augmented state-space model of the HDT is developed, incorporating the delays introduced by the digital control system and resonant states to eliminate steady-state errors. The control gains are optimized using PSO to minimize a cost function that considers both transient and steady-state performance. Simulation results demonstrate the effectiveness of the proposed control strategy in regulating the voltage and current of the HDT under various operating conditions.

Index Terms—hybrid distribution transformer, optimal control, state-feedback control, particle swarm optimization

I. INTRODUCTION

THE increasing penetration of renewable energy sources in the electrical grid has led to a significant rise in the use of power electronic converters. These converters are essential for integrating RES into the grid, as they facilitate the conversion of DC power generated by sources like solar panels and wind turbines into AC power compatible with the grid. However, the widespread use of power electronic converters has also introduced challenges related to power quality, such as the injection of harmonics and non-linear loads, which can lead to voltage distortions and other issues in the electrical grid.

There are many solutions that have been proposed to address the power quality issues in the grid, such as STATCOMs, the dynamic voltage restorers (DVRs) active power filters (APFs), the unified power quality conditioners (UPQC) and the solid-state transformers (SST). SSTs has the ability to mitigate most of the power quality issues mentioned above, while also providing galvanic isolation and voltage transformation. However, the high cost and complexity of SSTs has limited their widespread adoption in the distribution grid and, also,

does not provide the same short-circuit current capability as traditional distribution transformers (DTs).

For this reason, the hybrid distribution transformer (HDT) emerges as a promising solution to address the disadvantages of SSTs while still providing advanced power quality functionalities. The HDT is a power electronic transformer that combines the functions of a traditional distribution transformer with those of power electronic converters. Many HDT configurations have been proposed in the literature, and in consequence, classifications have been made [1]. One of the classifications is based on the source of the converter's energy, i.e., whether the energy is obtained from a capacitor/battery, the primary or secondary side of the DT, or an auxiliary winding. On the other hand, the other classification is based on how the converters inject energy into the system, i.e., whether they are connected in series or in parallel with the DT.

In this paper, the configuration of the HDT consists of the DT connected to two back-to-back voltage source converters (VSCs): a series converter connected to the primary of the DT through a coupling transformer (CT), and a parallel converter connected in parallel to the load, which is connected to the secondary of the DT. A circuit diagram of the HDT is shown in fig. 1. The series converter is responsible for regulating the voltage at the primary side of the DT, while the parallel converter is responsible for regulating the current injected into the load.

Several control strategies have been proposed for the HDT in the literature, including finite control set model predictive control (FC-MPC) [2], switching V-f and P-Q mode control [3], and decoupled control strategies, such as the resonant control [4] the compound controller [5], quasi-proportional controller [6] and the separated state-feedback controller [7].

In this paper, a unified control strategy based on state feedback control with resonant states is proposed for the HDT. This control strategy aims to achieve zero steady-state error for sinusoidal references and disturbances, while also

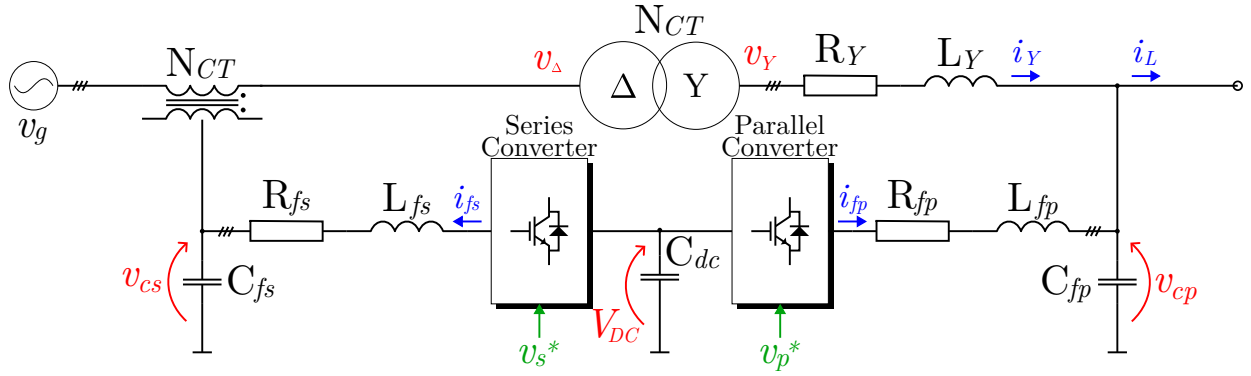


Fig. 1. Hybrid distribution transformer circuit diagram.

ensuring good dynamic performance. The control strategy is designed using an augmented state-space model of the HDT that includes the delays introduced by the digital control system and the resonant states to achieve zero steady-state error for sinusoidal references and disturbances. The control gains are optimized using particle swarm optimization (PSO) to minimize a cost function that considers both the transient and steady-state performance of the HDT. The proposed control strategy is validated through simulation results that demonstrate its effectiveness in regulating the voltage and current of the HDT under various operating conditions.

II. MODEL OF THE HYBRID DISTRIBUTION TRANSFORMER

A. Series Converter

The series converter dynamics are given by:

$$\begin{aligned} v_s^{abc} &= R_{fs} i_{fs}^{abc} + L_{fs} \frac{d i_{fs}^{abc}}{dt} + v_{cs}^{abc} \\ i_{fs}^{abc} &= C_{fs} \frac{d v_{cs}^{abc}}{dt} + i_g^{abc} \end{aligned} \quad (1)$$

where v_s^{abc} is the series converter output voltage, i_{fs}^{abc} is the series converter inductor current, v_{cs}^{abc} is the series converter output capacitor voltage, and i_g^{abc} is the grid current after the coupling transformer. The parameters R_{fs} , L_{fs} , and C_{fs} are the series converter filter resistance, inductance, and capacitance respectively.

Leaving the states on the left side, and converting to $\alpha\beta$ coordinates, the series converter model is given by:

$$\begin{aligned} \frac{d i_{fs}^{\alpha\beta}}{dt} &= -\frac{R_{fs}}{L_{fs}} i_{fs}^{\alpha\beta} - \frac{1}{L_{fs}} v_{cs}^{\alpha\beta} + \frac{1}{L_{fs}} v_s^{\alpha\beta} \\ \frac{d v_{cs}^{\alpha\beta}}{dt} &= -\frac{1}{C_{fs}} i_{fs}^{\alpha\beta} + \frac{1}{C_{fs}} i_g^{\alpha\beta} \end{aligned} \quad (2)$$

B. Parallel Converter

The parallel converter dynamics are given by:

$$\begin{aligned} v_p^{abc} &= R_{fp} i_{fp}^{abc} + L_{fp} \frac{d i_{fp}^{abc}}{dt} + v_{cp}^{abc} \\ i_{fp}^{abc} &= C_{fp} \frac{d v_{cp}^{abc}}{dt} - i_Y^{abc} + i_L^{abc} \end{aligned} \quad (3)$$

where v_p^{abc} is the parallel converter output voltage, i_{fp}^{abc} is the parallel converter inductor current, v_{cp}^{abc} is the parallel converter output capacitor voltage, i_Y^{abc} is the transformer Y side current, and i_L^{abc} is the load current. The parameters R_{fp} , L_{fp} , and C_{fp} are the parallel converter filter resistance, inductance, and capacitance respectively.

Leaving the states on the left side, and converting to $\alpha\beta$ coordinates, the series converter model is given by:

$$\begin{aligned} \frac{d i_{fp}^{\alpha\beta}}{dt} &= -\frac{R_{fp}}{L_{fp}} i_{fp}^{\alpha\beta} - \frac{1}{L_{fp}} v_{cp}^{\alpha\beta} + \frac{1}{L_{fp}} v_p^{\alpha\beta} \\ \frac{d v_{cp}^{\alpha\beta}}{dt} &= \frac{1}{C_{fp}} i_{fp}^{\alpha\beta} - \frac{1}{C_{fp}} i_Y^{\alpha\beta} + \frac{1}{C_{fp}} i_L^{\alpha\beta} \end{aligned} \quad (4)$$

C. Distribution Transformer

The transformer is connected in $\Delta - Y$ configuration, with the series converter (through the coupling transformer) connected to the Δ side, and the parallel converter connected to the Y side. The Y side has its neutral point grounded. The transformer equations are given by:

$$\begin{aligned} v_{YA} &= N_{LFT}(v_{\Delta a} - v_{\Delta b}) \\ v_{YB} &= N_{LFT}(v_{\Delta b} - v_{\Delta c}) \\ v_{YC} &= N_{LFT}(v_{\Delta c} - v_{\Delta a}) \end{aligned} \quad (5)$$

This can be expressed in matrix form as:

$$v_Y^{abc} = N_{LFT} \underbrace{\begin{bmatrix} 1 & -1 & 0 \\ 0 & 1 & -1 \\ -1 & 0 & 1 \end{bmatrix}}_{K'_T} v_\Delta^{abc} \quad (6)$$

$$v_Y^{abc} = N_{LFT} K'_T v_\Delta^{abc}$$

In the other hand, the dynamics of the transformer are modeled as a series impedance referred to the Y side. These transformer equations are given by:

$$v_Y^{abc} = R_Y i_Y^{abc} + L_Y \frac{d i_Y^{abc}}{dt} + v_{cp}^{abc} \quad (7)$$

Assuming that there is no zero-sequence current, and using the expression given in (6), the transformer model can be expressed in $\alpha\beta$ coordinates as:

$$\frac{d i_Y^{\alpha\beta}}{dt} = -\frac{R_Y}{L_Y} i_Y^{\alpha\beta} - \frac{1}{L_Y} v_{cp}^{\alpha\beta} + \frac{1}{L_Y} N_{LFT} K'_T v_{\Delta}^{\alpha\beta} \quad (8)$$

D. Overall HDT Model

The overall HDT model can be expressed in state-space form as:

$$\begin{aligned} \frac{d}{dt} \begin{bmatrix} x_s \\ x_p \end{bmatrix} &= \underbrace{\begin{bmatrix} \mathbf{A}_s & \mathbf{P}_{ig} \mathbf{M}_p \\ \mathbf{P}_{vc} \mathbf{M}_s & \mathbf{A}_p \end{bmatrix}}_{\mathbf{A}} \begin{bmatrix} x_s \\ x_p \end{bmatrix} + \underbrace{\begin{bmatrix} \mathbf{B}_s & \mathbf{0} \\ \mathbf{0} & \mathbf{B}_p \end{bmatrix}}_{\mathbf{B}} \begin{bmatrix} u_s \\ u_p \end{bmatrix} \\ &+ \underbrace{\begin{bmatrix} \mathbf{0} \\ \mathbf{P}_{vg} \end{bmatrix}}_{\mathbf{P}_{vg}} v_g + \underbrace{\begin{bmatrix} \mathbf{0} \\ \mathbf{P}_{iL} \end{bmatrix}}_{\mathbf{P}_{iL}} i_L \end{aligned} \quad (9)$$

where the matrices $\mathbf{M}_p = [\mathbf{0} \quad \mathbf{I} \quad \mathbf{0}]$ and $\mathbf{M}_s = [\mathbf{0} \quad \mathbf{I}]$ are used to select the appropriate states from the parallel and series converter state vectors respectively.

The last can be expressed in a more compact form as:

$$\begin{aligned} \frac{dx(t)}{dt} &= \mathbf{Ax}(t) + \mathbf{Bu}(t) + \mathbf{P}_{vg} v_g(t) + \mathbf{P}_{iL} i_L(t) \quad (10) \\ y(t) &= \mathbf{Cx}(t) \end{aligned}$$

with the states $x(t) = [i_{fs}^{\alpha\beta} \quad v_{cs}^{\alpha\beta} \quad i_{fp}^{\alpha\beta} \quad i_Y^{\alpha\beta} \quad v_{cp}^{\alpha\beta}]^T$, input $u(t) = [v_s^{\alpha\beta} \quad v_p^{\alpha\beta}]^T$, and output $y(t) = [i_{fs}^{\alpha\beta} \quad v_{cs}^{\alpha\beta} \quad i_{fp}^{\alpha\beta} \quad i_Y^{\alpha\beta} \quad v_{cp}^{\alpha\beta}]^T$.

The HDT system is discretized using a zero-order hold with a sampling time of $T_s = 5 \mu s$. The discrete-time state-space model is given by:

$$\begin{aligned} x[k+1] &= \mathbf{A}_d x[k] + \mathbf{B}_d u[k] + \mathbf{P}_{vg,d} v_g[k] + \mathbf{P}_{iL,d} i_L[k] \\ y[k] &= \mathbf{C} x[k] \end{aligned} \quad (11)$$

where $\mathbf{A}_d = e^{\mathbf{A} T_s}$, $\mathbf{B}_d = \int_0^{T_s} e^{\mathbf{A}\tau} d\tau \mathbf{B}$, $\mathbf{P}_{vg,d} = \int_0^{T_s} e^{\mathbf{A}\tau} d\tau \mathbf{P}_{vg}$, $\mathbf{P}_{iL,d} = \int_0^{T_s} e^{\mathbf{A}\tau} d\tau \mathbf{P}_{iL}$, and $\mathbf{C} = \mathbb{I}$.

In most of the applications, there is a delay of one sampling period between the calculation of the control input and its application to the system. To account for this delay, the discrete-time state-space model is augmented with a new state representing the previous control input:

$$m_k = u_{k-1} \quad (12)$$

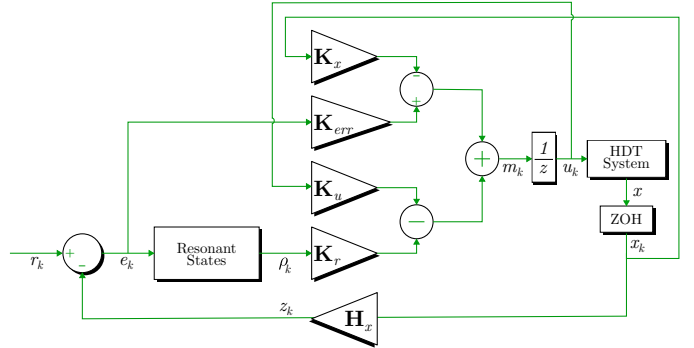


Fig. 2. Block diagram of the proposed control strategy for the HDT.

This can be expressed in state-space form as:

$$\begin{bmatrix} x_{k+1} \\ m_{k+1} \end{bmatrix} = \underbrace{\begin{bmatrix} \mathbf{A}_d & \mathbf{B}_d \\ \mathbf{0} & \mathbf{0} \end{bmatrix}}_{\mathbf{A}_{d,\text{delay}}} \begin{bmatrix} x_k \\ m_k \end{bmatrix} + \underbrace{\begin{bmatrix} \mathbf{0} \\ \mathbf{I} \end{bmatrix}}_{\mathbf{B}_{d,\text{delay}}} u_k \quad (13)$$

III. CONTROL STRATEGY

With the state-space model of the HDT defined, the next step is to design a control strategy that ensures the desired performance. The proposed control strategy is based on a state feedback controller with integral action and resonant states to achieve zero steady-state error for sinusoidal references and disturbances. The block diagram of the proposed control strategy is shown in Fig. 2.

$$u_k = -\mathbf{K}_x \mathbf{H}_a \begin{bmatrix} x_k \\ m_k \end{bmatrix} + \mathbf{K}_{err} e_k - \mathbf{K}_r \rho_k + \mathbf{K}_u m_k \quad (14)$$

where \mathbf{K}_x is the state feedback gain matrix, \mathbf{H}_a is the matrix that selects the states without reference, \mathbf{K}_{err} is the error gain matrix, e_k is the error vector, \mathbf{K}_r is the resonant states gain matrix, ρ_k is the resonant states vector, \mathbf{K}_u is the previous control input gain matrix, and u_{k-1} is the previous control input vector.

The resonant states are included to ensure zero steady-state error for sinusoidal references and disturbances. The resonant states dynamics are given by:

$$\frac{d \rho(t)}{dt} = \underbrace{\begin{bmatrix} -2\xi\omega & \omega \\ -\omega & 0 \end{bmatrix}}_{\mathbf{A}_r} \rho(t) + \underbrace{\begin{bmatrix} 1 \\ 0 \end{bmatrix}}_{\mathbf{B}_r} e(t) \quad (15)$$

where ω is the nominal angular frequency, ξ is the damping factor. Each of the references signals has two resonant states associated with it, meaning that for the HDT control, there are eight resonant states in total (4 for the $v_{cs,\alpha\beta}$ and 4 for the $i_{fp,\alpha\beta}$). This can be expressed as:

$$\frac{d \rho(t)}{dt} = \text{blkdiag}(\mathbf{A}_r, \mathbf{A}_r, \mathbf{A}_r, \mathbf{A}_r) \rho(t) \quad (16)$$

$$+ \text{blkdiag}(\mathbf{B}_r, \mathbf{B}_r, \mathbf{B}_r, \mathbf{B}_r) e(t) \quad (17)$$

These resonant states are then discretized using a ZOH giving the matrices \mathbf{A}_{rd} and \mathbf{B}_{rd} . The augmented state-space model of the resonant states can be expressed as:

$$\begin{bmatrix} x_{k+1} \\ m_{k+1} \\ \rho_{k+1} \end{bmatrix} = \begin{bmatrix} \mathbf{A}_{d,delay} & \mathbf{0} \\ \mathbf{B}_{rd} \mathbf{H}_x & \mathbf{A}_{rd} \end{bmatrix} \begin{bmatrix} x_k \\ m_k \\ \rho_k \end{bmatrix} + \begin{bmatrix} \mathbf{B}_{d,aug} \\ \mathbf{0} \end{bmatrix} \begin{bmatrix} u_k \\ e_k \end{bmatrix} \quad (18)$$

$$y_k = [\mathbf{C} \quad \mathbf{0}] \begin{bmatrix} x_K \\ m_k \\ \rho_k \end{bmatrix}$$

where \mathbf{H}_x selects the states from the HDT state vector that are imposed to follow references.

A. Particle Swarm Optimization

The PSO algorithm is a population-based optimization technique inspired by the social behavior of birds and fish. It consists of a swarm of particles, where each particle represents a potential solution to the optimization problem. The particles move through the search space, updating their positions based on their own experience and the experience of their neighbors. The velocity and position of each particle are updated using the following equations:

$$\begin{aligned} v_j(i+1) &= K_{ap} (v_j(i) + c_1 r_1 (pbest_j - x_j(i)) \\ &\quad + c_2 r_2 (gbest - x_j(i))) \end{aligned} \quad (19)$$

$$x_j(i+1) = x_j(i) + v_j(i+1)$$

where $v_j(i)$ is the velocity of particle j at iteration i , $x_j(i)$ is the position of particle j at iteration i , $pbest_j$ is the best position found by particle j , $gbest$ is the best position found by the entire swarm, c_1 and c_2 are cognitive and social acceleration coefficients, r_1 and r_2 are random numbers uniformly distributed in the range $[0, 1]$, and K_{ap} is the constriction factor given by:

$$K_{ap} = \frac{2}{|2 - \phi - \sqrt{\phi^2 - 4\phi}|} \quad (20)$$

where $\phi = c_1 + c_2 > 4$ is a constant that ensures convergence.

The PSO algorithm iteratively updates the positions and velocities of the particles until a stopping criterion is met, such as a maximum number of iterations or a satisfactory solution. The best position found by the swarm is considered the optimal solution to the optimization problem.

IV. SIMULATION RESULTS

In this section, the simulation results of the proposed control strategy are presented. The simulations are performed using MATLAB/Simulink, and the system parameters are listed in Table I. The proposed control strategy is tested under various grid and load disturbances, including grid voltage unbalanced swell, load impact, and unbalanced load.

A. Grid Voltage Unbalanced Swell Compensation

The simulation results for the proposed control strategy under grid voltage unbalanced swell are shown in Fig. 3. The grid voltage swell occurs at $t = 0.02$ s and lasts for 0.08 s. The proposed control strategy effectively compensates for the voltage swell, maintaining a balanced load current.

TABLE I
SYSTEM PARAMETERS

Parameter	Variable	Value
Grid Voltage	V_g	10 kV
Grid Frequency	f_e	50 Hz
Transformers Power Rating	S	1 kVA
DC Link Voltage	V_{DC}	400 V
Series Converter Filter Inductance	L_{fs}	2 mH
Series Converter Filter Capacitance	C_{fs}	20 μ F
Parallel Converter Filter Inductance	L_{fp}	2 mH
Parallel Converter Filter Capacitance	C_{fp}	20 μ F
Transformer Dispersion Inductance	L_Y	0.1 mH
Transformer Series Resistance	R_Y	50 Ω
Coupling Transformer Turns Ratio	N_{ct}	2.5
Distribution Transformer Turns Ratio	N_{DT}	a
Converters Switching Frequency	f_{sw}	20 kHz
Control Sampling Time	T_s	5 μ s

B. Load Impact and Unbalanced Load Compensation

In the other hand, a load unbalance is applied at $t = 0.1$ s and lasts for 0.06 s. Then, an unbalanced load is applied at $t = 0.16$ s and lasts for 0.06 s. The proposed control strategy effectively compensates for the load unbalance, meaning that the parallel inverter injects the necessary current to maintain a balanced load current, as shown in Fig. 4.

V. CONCLUSIONS

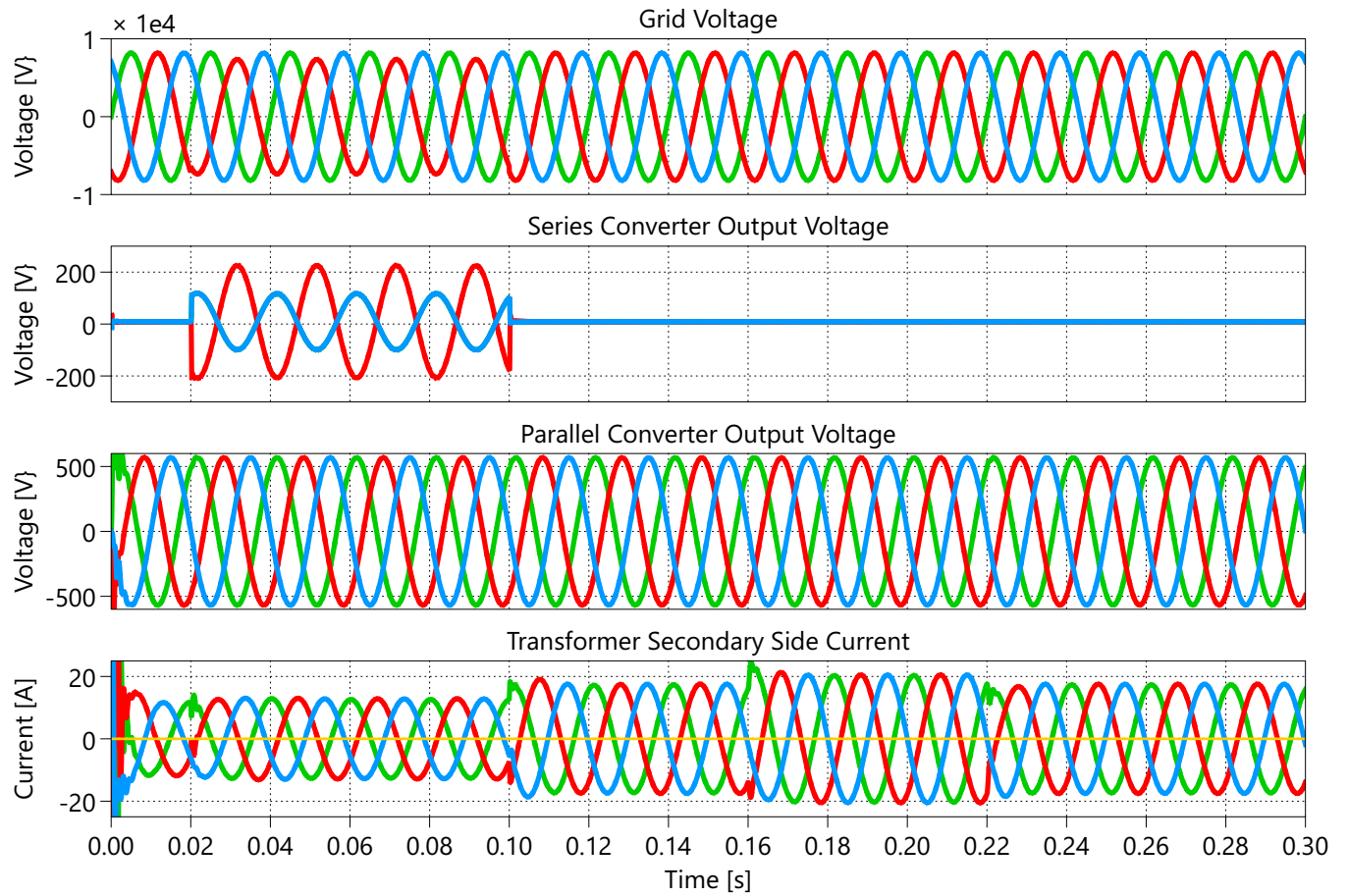


Fig. 3. Simulation results for the proposed control strategy under grid and load disturbances.

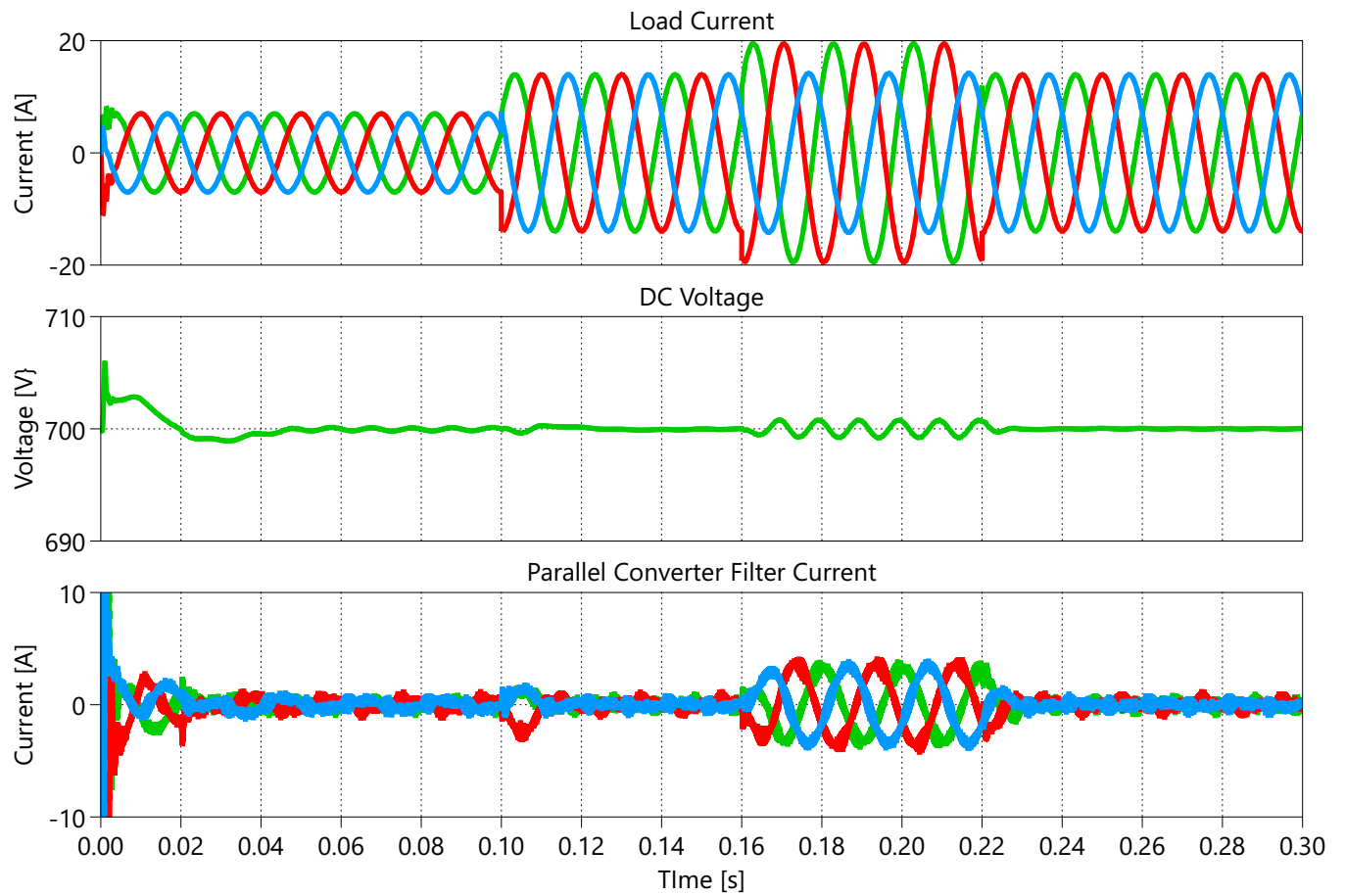


Fig. 4. Simulation results for the proposed control strategy under grid and load disturbances.

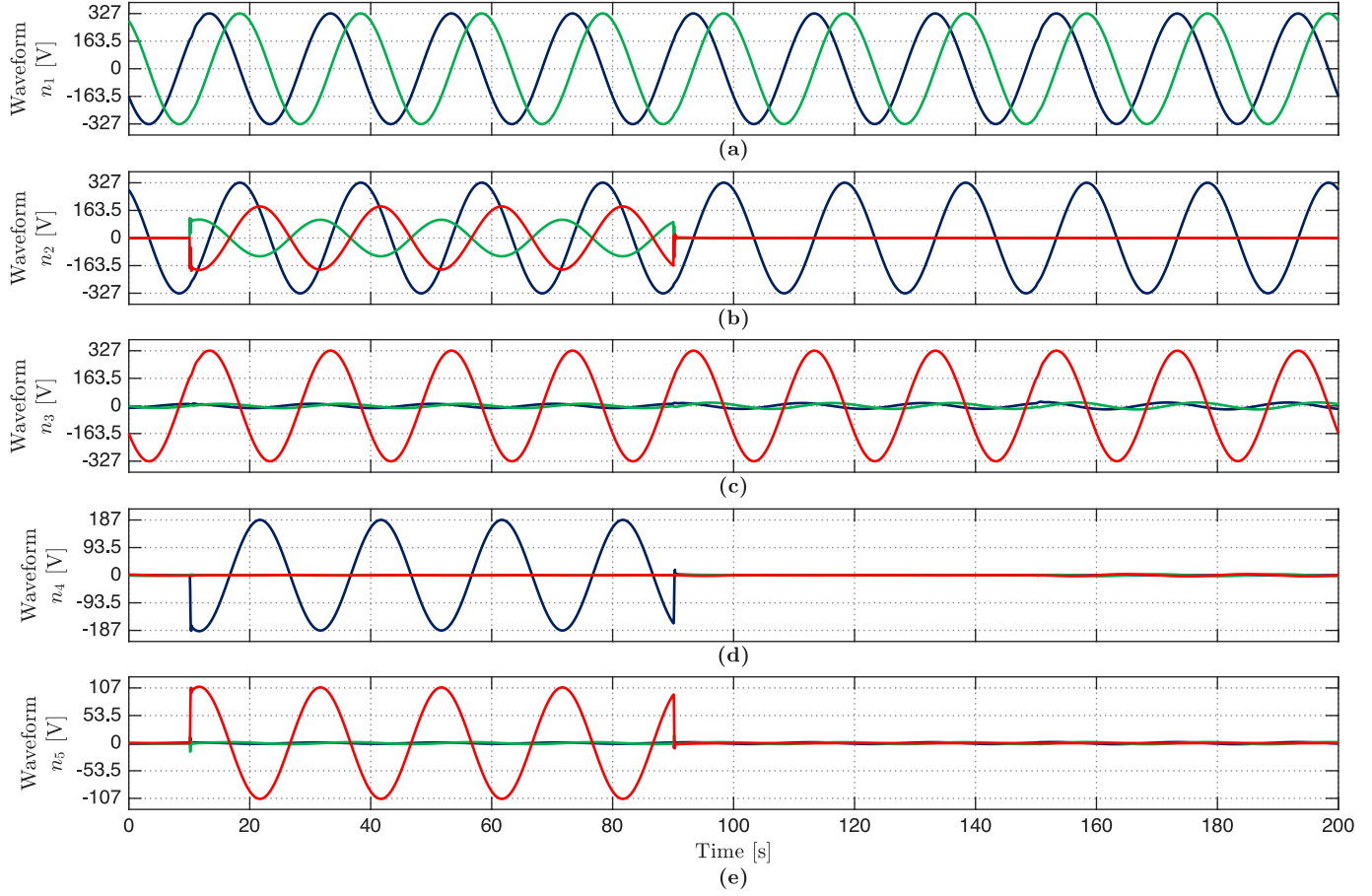


Fig. 5. Simulation results for the proposed control strategy under grid and load disturbances.

REFERENCES

- [1] A. Carreno, M. Perez, C. Baier, A. Huang, S. Rajendran, and M. Malinowski, "Configurations, Power Topologies and Applications of Hybrid Distribution Transformers," *Energies*, vol. 14, no. 5, p. 1215, Feb. 2021.
- [2] P. Costa, G. Paraíso, S. F. Pinto, and J. F. Silva, "A four-leg matrix converter based hybrid distribution transformer for smart and resilient grids," *Electric Power Systems Research*, vol. 203, p. 107650, Feb. 2022.
- [3] X. Xu, Z. Qiu, T. Zhang, and H. Gao, "A Three-Phase Hybrid Transformer Topology and Its Control Strategy for Active Distribution Networks," in *2023 IEEE 7th Conference on Energy Internet and Energy System Integration (EI2)*, Dec. 2023, pp. 643–649.
- [4] W. Matelski, "Badania eksperymentalne transformatora hybrydowego jako kondycjonera napięcia w sieciach typu TN," *PRZEGŁĄD ELEKTROTECHNICZNY*, vol. 1, no. 5, pp. 233–238, May 2023.
- [5] Y. Liu, D. Liang, P. Kou, M. Zhang, S. Cai, K. Zhou, Y. Liang, Q. Chen, and C. Yang, "Compound Control System of Hybrid Distribution Transformer," *IEEE Transactions on Industry Applications*, vol. 56, no. 6, pp. 6360–6373, Nov. 2020.
- [6] Y. Liu, L. Zhang, D. Liang, H. Jin, S. Li, S. Jia, J. Li, H. Liu, Y. Wang, K. Zhou, Y. Gao, S. Cai, D. Li, and S. Feng, "Quasi-Proportional-Resonant Control for the Hybrid Distribution Transformer With LCL-Type Converters," *IEEE Transactions on Industry Applications*, vol. 58, no. 5, pp. 6368–6385, Sep. 2022.
- [7] A. Carreno, M. A. Perez, and M. Malinowski, "State-Feedback Control of a Hybrid Distribution Transformer for Power Quality Improvement of a Distribution Grid," *IEEE Transactions on Industrial Electronics*, vol. 71, no. 2, pp. 1147–1157, Feb. 2024.